Materials Letters. Vol. 62. Núm. 4-5. 2008. Pag. 780-783
http://dx.doi.org/10.1016/j.matlet.2007.06.067

High temperature coercivity of Nb containing hitperm alloys: Effect of Cu addition.

J. S. Blázquez[a], V. Franco[a], C.F. Conde[a], A. Conde[a]*, J. Ferenc[b] and T. Kulik[b]

[a]Dpto. Física de la Materia Condensada, ICMSE-CSIC, Universidad de Sevilla, P.O. Box 1065, 41080, Sevilla, Spain

[b]Faculty of Materials Science and Engineering, Warsaw University of Technology, ul. Wołoska 141, 02-507 Warsaw, Poland

ABSTRACT: Hysteresis loops of nanocrystalline samples of $Fe_{39}Co_{39}Nb_6B_{16-y}Cu_y$ (y = 0, 1) HITPERM-type alloys were measured from room temperature up to 773 K. The alloy with Cu shows a nearly constant value of coercivity (~ 135 A/m) in all the studied temperature range, whereas for the Cu-free alloy, the coercivity increases from 125 A/m at 300 K up to 190 A/m at 773 K. Room temperature Mössbauer spectra can be interpreted on the basis of the presence of three different regions: amorphous, crystalline and interface. The observed nanocrystalline microstructure is similar for the two alloys, although bigger crystallites are found in the alloy without Cu. The very small grain size ensures the averaging out of the magnetocrystalline anisotropy but, as the expected value of magnetostriction constant for the crystalline phase is ~ 60 ppm, the magnetoelastic anisotropy can not be neglected.

*Corresponding author: Prof. A. Conde

Departamento de Física de la Materia Condensada. Universidad de Sevilla.

Apartado 1065, 41080 Sevilla (Spain).

Phone: (34) 95 455 28 85

Fax: (34) 95 461 20 97

E-mail: conde@us.es

Materials Letters. Vol. 62. Núm. 4-5. 2008. Pag. 780-783
http://dx.doi.org/10.1016/j.matlet.2007.06.067

1 Introduction

The microstructure of the nanocrystalline Fe-based soft magnetic alloys (crystallites of about 10 nm embedded in a residual amorphous matrix) is the responsible for their outstanding soft magnetic properties by averaging out the magnetocrystalline anisotropy [1]. These alloys can be divided into two compositions: FINEMET (with Si) [2] and NANOPERM (without Si) [3]. Both systems exhibit exceptional soft magnetic properties at room temperature [4]. However, the Curie temperature of the amorphous phase, T_C^{am}, marks a limit for the technological application of these alloys at high temperature due to the magnetic uncoupling of the nanocrystals at temperatures above T_C^{am}. In order to solve this limitation, HITPERM alloys were developed [5]. In these alloys, T_C^{am} increases due to the partial substitution of Co for Fe.

The effect of the addition of a small amount of Cu is known to be different for Nb and Zr containing HITPERM alloys, being useless in the case of Zr-HITPERM [6] but refining the microstructure through Cu-clustering phenomenon in Nb-containing HITPERM alloys [7] as it occurs for FINEMET [8] and Co-free NANOPERM [9] alloys.

Soft magnetic properties of several HITPERM alloys at temperatures above 300 K have been reported on saturation magnetization [5] and initial susceptibility [10]. Their low coercivity yields the lack of data on hysteresis loop at elevated temperatures of these systems and just a few studies have been published in the last two years [11,12,13,14].

Materials Letters. Vol. 62. Núm. 4-5. 2008. Pag. 780-783
http://dx.doi.org/10.1016/j.matlet.2007.06.067

In this work, the high temperature soft magnetic properties of two nanocrystalline $Fe_{39}Co_{39}Nb_6B_{16-y}Cu_y$ (y = 0, 1) HITPERM-type alloys are studied and correlated with the differences in the microstructure due to the addition of 1 at. % of Cu.

2 Experimental

Ribbons of the two compositions were produced by the melt-spinning technique (~5 mm wide and ~20 μm thick). Thermomagnetic gravimetry (TMG) performed in a Perkin-Elmer TGA-7, applying to the sample the magnetic field of a small magnet (~20 mT), was used to characterize the magnetic transitions of the system. Mössbauer spectra (MS) were recorded at room temperature in a transmission geometry using a ^{57}Co(Rh) source to characterize the local environment of Fe in nanocrystalline and amorphous samples. The incident γ-beam was perpendicular to the ribbon plane. The values of the hyperfine parameters were obtained by fitting with NORMOS program [15]. The isomer shift, *IS*, was quoted relative to an α-Fe foil at room temperature. The spectra of amorphous samples were fitted using a distribution of hyperfine magnetic fields, DHF. In the case of nanocrystalline samples, a set of discrete values of hyperfine magnetic fields, H, and two DHFs were used to fit the experimental data. The two DHFs would roughly correspond to the amorphous phase (from 0 to 30 T) and the interface region (from 14.5 to 32.5 T). As the limit between magnetic hyperfine fields corresponding to the interface and to the amorphous regions is not sharp, overlapping was allowed in a wide range of hyperfine magnetic fields. The quadrupolar splitting was negligible. High temperature hysteresis loops were recorded using a quasistatic hysteresis loop tracer. The dc field was applied using two Helmholtz coils outside the furnace. The sample and the pick up coil were introduced into the furnace.

Materials Letters. Vol. 62. Núm. 4-5. 2008. Pag. 780-783
http://dx.doi.org/10.1016/j.matlet.2007.06.067

The loops were acquired by using a continuous heating rate low enough to assure that during the acquisition time of each loop the temperature rises less than 3 K. After the measurements at high temperature, the samples were measured again at room temperature and no significant change in coercivity was found indicating no microstructural evolution of the samples during the measurement at high temperature. The values of magnetization, M, were rescaled using the value obtained at room temperature and 0.5 T in a vibrating sample magnetometer, VSM (Lakeshore 7407).

3 Results and discussion

Figure 1 shows the TMG plots of as-cast samples of the two studied alloys. The arrow indicates the temperature up to which the samples were heated to develop the nanocrystalline microstructure. The first fall of M is due to the ferro-paramagnetic transition of the amorphous alloy. This fall does not reach zero but overlaps with the rise of M due to the formation of the α-Fe nanocrystals. The overlapping is stronger for the alloy with Cu, as this alloy exhibits a lower crystallization temperature. The second fall is ascribed to a partial recrystallization of the α-Fe crystallites and the residual amorphous matrix [16].

Figure 2 shows the experimental as well as the fitted MS spectra for the two studied nanocrystalline alloys. The contribution of the pure crystalline sites and those of the two distributions are also shown. Figure 3 shows the probability distribution of the hyperfine magnetic field contributions of the two DHFs and the two Fe sites used in the fitting. The values of the DHF corresponding to the interface region are negligible below 25 T. The main results obtained from the MS data are shown in table 1. The average *H* and *IS* values of the crystalline sites are almost the same for both compositions (34.7 T and 0.028 mm/s, respectively) showing no significant differences

in the composition or the degree of order in the crystalline phase between the two studied alloys. The values of the isomer shift of the crystalline and interface sites are similar (0.028 and 0.023 mm/s respectively) but clearly different to those of the amorphous sites (> 0.100 mm/s). From the fraction of Fe atoms in crystalline and interface sites, it is possible to estimate the nanocrystal size of the two compositions from:

$$D = 2\delta \frac{\sqrt[3]{\frac{A_I}{A_C} + 1}}{\sqrt[3]{\frac{A_I}{A_C} + 1} - 1}$$

where δ is the interface thickness (region constituted by atoms in the crystalline lattice but which hyperfine field is affected by atoms outside the lattice), A_I is the fraction of Fe atoms at the interface and A_C is the fraction of Fe atoms ascribed to inner sites of the crystallites. The value of the grain size of the alloy without Cu, D^{MS}_{0-Cu} being 1.3 times bigger than that of the alloy with Cu, D^{MS}_{1-Cu}, if a similar δ is assumed. Transmission electron microscopy studies on these alloys [17] show that the average size of nanocrystals are ~5 and ~7.5 nm for the alloy with Cu and without Cu, respectively and $D^{TEM}_{0-Cu} / D^{TEM}_{1-Cu}$ = 1.5, in agreement with the results of the present paper. The thickness of the interface layer could be estimated as 0.2-0.3 nm.

Figure 4 shows some representative hysteresis loops measured at different temperatures for both studied alloys. Figure 5 shows the coercivity, H_C, and the specific magnetization, σ_S, as a function of the temperature of measurement. For the alloy with Cu, an almost constant value of H_C can be observed in all the studied range. However, for the alloy without Cu, H_C increases from 120 A/m at room temperature up to 190 A/m at 700 K, remaining almost constant up to the end of the temperature range of the

experiment. These values of coercivity are larger than those of conventional nanocrystalline alloys at room temperature, although the size of the crystallites is similar in the studied alloys and thus should enable an effective averaging out of magnetocrystalline anisotropy. However, the magnetostriction of HITPERM alloys increases due to the high value of the magnetostriction of α-FeCo phase (60 ppm) [18]. Therefore, magnetoelastic anisotropy is the responsible for the higher values of H_C observed at room temperature for HITPERM alloys with respect to conventional nanocrystalline systems. Magnetization continuously decreases for both alloys from 145 and 130 emu/g (at room temperature, for Cu-free and Cu-containing alloy, respectively) down to 110 emu/g at 700 K, being constant for higher temperatures. It is worth noting that the Curie temperature of the amorphous alloy could be of about this temperature (as estimated from Fig. 1). Therefore, the magnetic properties of the alloy without Cu are more sensitive to the thermal approach to the magnetic transition of the amorphous phase than those of the Cu containing alloy.

Both alloys show a similar crystalline fraction and a similar magnetostriction, but different average grain size and thus a different value of the amorphous layer thickness between two neighbor nanocrystals. The increase in coercivity could be ascribed to a reduction in the magnetic coupling between nanocrystals as the amorphous matrix approaches its magnetic transition. The presence of Cu refines the microstructure of the alloy and decreases the thickness of the amorphous layer between nanocrystals. Therefore, as the average distance between nanocrystals is smaller in the alloy with Cu, it is not surprising that the magnetic coupling between them is less sensitive to the approach to T_C^{am}. In fact, for the same crystalline fraction, the coupling between nanocrystals is enhanced if the distance between nanocrystals is reduced as shown by

theoretical [1] and experimental results. For example, the refinement of the microstructure can be achieved by Joule heating [19]. The relative decrease of the magnetization is also larger in the Cu-free alloy (24 %) than in the alloy with Cu (15 %) supporting the stronger sensitiveness of the Cu-free alloy to the temperature as it approaches T_C^{am}.

Conclusions

The addition of 1 at. % of Cu to the HITPERM alloy $Fe_{39}Co_{39}Nb_6B_{16}$ refines the final nanocrystalline microstructure, unlike for Zr-containing HITPERM alloys. As the same crystalline volume fraction is achieved at the end of the nanocrystallization, this yields a reduced thickness of the amorphous layer between neighbour nanocrystals. This difference could be responsible for the stronger sensitiveness to the Curie transition of the residual amorphous matrix observed in the thermal dependence of the magnetic properties of the Cu-free alloy.

Acknowledgements

This work was supported by the Spanish Government and EU FEDER (Project MAT 2004-04618), the PAI of the Junta de Andalucía and the Centre of Excellence NanoCentre. J.S.B. acknowledges a research contract from this regional government.

Materials Letters. Vol. 62. Núm. 4-5. 2008. Pag. 780-783
http://dx.doi.org/10.1016/j.matlet.2007.06.067

References

[1] A. Hernando, M. Vázquez, T. Kulik, C. Prados, Phys. Rev. B 51 (1995) 3581.
[2] Y. Yoshizawa, S. Oguma, and K. Yamauchi, J. Appl. Phys. 64, (1988) 6044.
[3] K. Suzuki, A. Makino, N. Kataoka, A. Inoue, T. Masumoto, Mater. Trans. JIM 32 (1991) 93.
[4] McHenry ME, Willard MA, Laughlin DE. Prog Mater Sci 1999; 44: 291
[5] M.E. McHenry, M.A. Willard, D.E. Laughlin, Progress in Mater. Sci. 44 (1999) 291.
[6] D.H. Ping, Y.Q. Wu, K. Hono, M.A. Willard, M.E. McHenry, D.E. Laughlin, Scripta Mater. 45 (2001) 781.
[7] Y. Zhang, J.S. Blázquez, A. Conde, P.J. Warren, A. Cerezo, Mat. Sci. Eng. A 353 (2003) 158
[8] Finemet Cu-cluster
[9] Nanoperm CU-cluster
[10] J.S. Blázquez, V. Franco, A. Conde, L.F. Kiss, J. Appl. Phys. 93 (2003) 2172.
[11] F. Mazaleyrat, Zs. Gercsi, J. Ferenc, T. Kulik, L.K. Varga, Mat. Sci. Eng. A 375-377 (2004) 1110.
[12] M. Kowalczyk, J. Ferenc, X.B. Liang, T. Kulik, J. Magn. Magn. Mat.304 (2006) e651.
[13] Mazaleyrat
[14] otro
[15] R. A. Brand, J. Lauer, D. M. Herlach, J. Phys. F: Met. Phys. 13 (1983) 675.
[16] J. S. Blázquez, C. F. Conde, A. Conde, Appl. Phys. Letters 79 (2001) 2898.
[17] J. S. Blázquez, V. Franco, A. Conde, J. Phys.: Condens. Matter 14 (2002) 11717.
[18] J. S. Blázquez, V. Franco, A. Conde, M. R. J. Gibbs, H. A. Davies, Z. C. Wang, J. Magn. Magn. Mat. 250 (2002) 260.
[19] R. Houssa, V. Franco, A. Conde, J. Magn. Magn. Mat. 203 (1999) 199.

Materials Letters. Vol. 62. Núm. 4-5. 2008. Pag. 780-783
http://dx.doi.org/10.1016/j.matlet.2007.06.067

Table 1: Results obtained from Mössbauer spectra.

Cu content	Fe sites	Area (%) ± 0.1	*H* (T) ± 0.1	<*H*> (T) ± 0.1	*IS* (mm/s) ± 0.005	<*IS*> (mm/s) ± 0.005
1 at. %	pure crystalline	20	34.0	34.6	0.037	0.029
		31	34.9		0.023	
	interface	18		29.2		0.023
	amorphous	31		12.2		0.111
0 at. %	pure crystalline	26	34.2	34.7	0.034	0.028
		27	35.2		0.022	
	interface	14		29.6		0.024
	amorphous	33		12.4		0.124

Materials Letters. Vol. 62. Núm. 4-5. 2008. Pag. 780-783
http://dx.doi.org/10.1016/j.matlet.2007.06.067

Figure captions

Fig. 1. TMG plots of as-cast samples of the two studied alloys.

Fig. 2. Mössbauer spectra and distribution of magnetic hyperfine field of annealed samples.

Fig. 3. Distribution probability of the hyperfine field contributions of the two studied alloys.

Fig. 4. Hysteresis loops measured at different temperatures for both studied nanocrystalline alloys.

Fig. 5. Coercivity and magnetization values of nanocrystalline samples as a function of the measuring temperature.

Materials Letters. Vol. 62. Núm. 4-5. 2008. Pag. 780-783
http://dx.doi.org/10.1016/j.matlet.2007.06.067

Figure 1

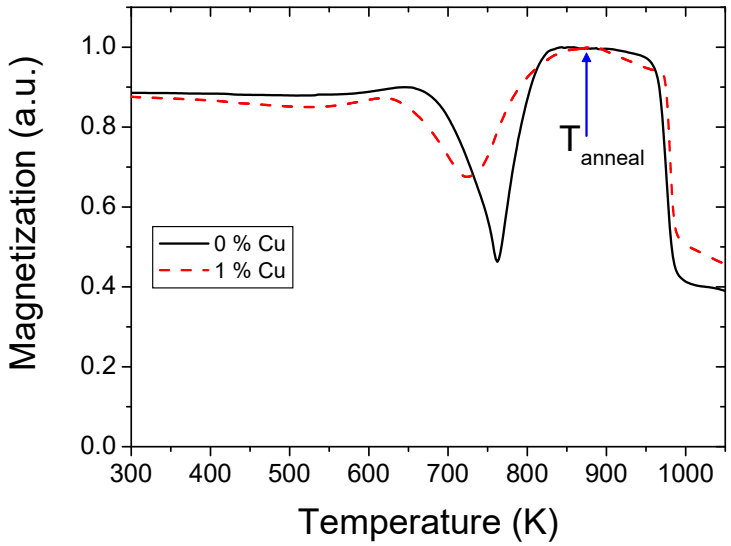

Materials Letters. Vol. 62. Núm. 4-5. 2008. Pag. 780-783
http://dx.doi.org/10.1016/j.matlet.2007.06.067

Figure 2

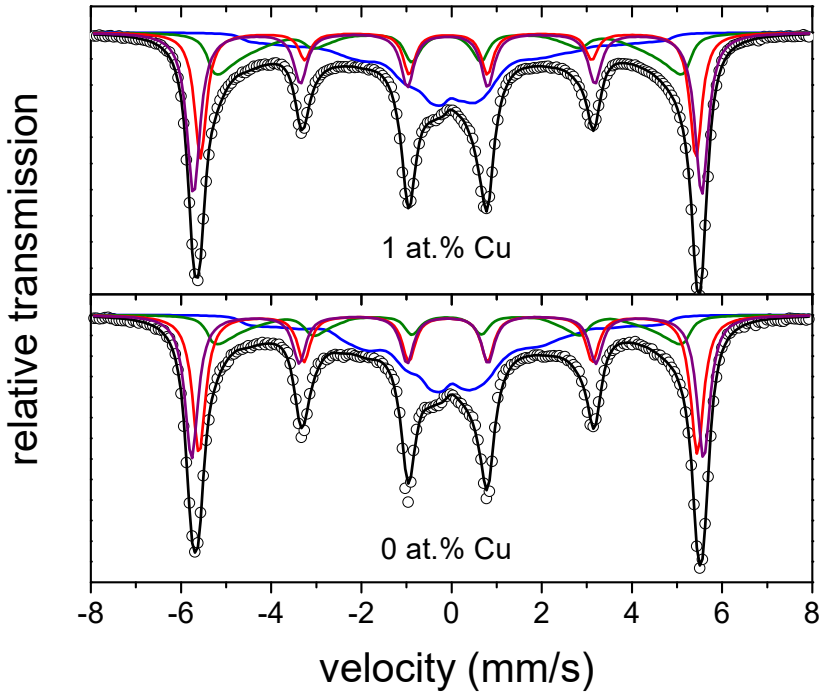

Materials Letters. Vol. 62. Núm. 4-5. 2008. Pag. 780-783
http://dx.doi.org/10.1016/j.matlet.2007.06.067

Figure 3

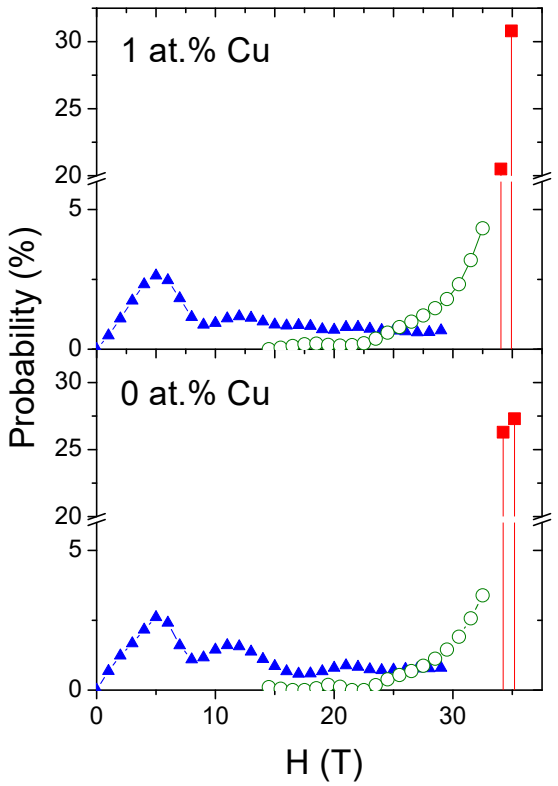

Materials Letters. Vol. 62. Núm. 4-5. 2008. Pag. 780-783
http://dx.doi.org/10.1016/j.matlet.2007.06.067

Figure 4

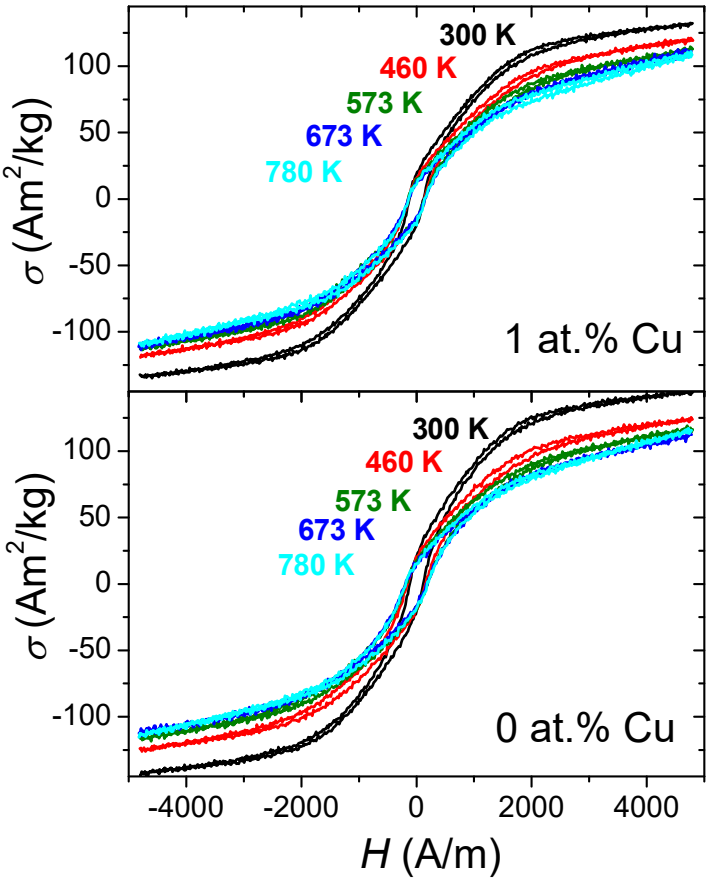

Materials Letters. Vol. 62. Núm. 4-5. 2008. Pag. 780-783
http://dx.doi.org/10.1016/j.matlet.2007.06.067

Figure 5